

AD A 039486

TECHNICAL REPORT TE-CR-77-2

COMPUTER SIMULATION OF TURBULENCE-INDUCED
POINTING JITTER FOR A LASER DESIGNATOR

Optical Science Consultants
P. O. Box 448
Placentia, California 92670

1 February 1977

Approved for public release; distribution unlimited.

Prepared for

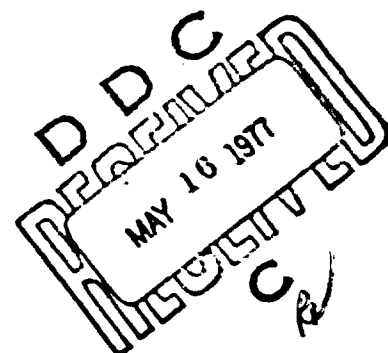
Advanced Sensors Directorate
Technology Laboratory

US Army Missile Research and Development Command
Redstone Arsenal, Alabama 35809

AD No. _____

DDC FILE COPY

(9) NW



DISPOSITION INSTRUCTIONS

DESTROY THIS REPORT WHEN IT IS NO LONGER NEEDED. DO NOT RETURN IT TO THE ORIGINATOR.

DISCLAIMER

THE FINDINGS IN THIS REPORT ARE NOT TO BE CONSTRUED AS AN OFFICIAL DEPARTMENT OF THE ARMY POSITION UNLESS SO DESIGNATED BY OTHER AUTHORIZED DOCUMENTS.

TRADE NAMES

USE OF TRADE NAMES OR MANUFACTURERS IN THIS REPORT DOES NOT CONSTITUTE AN OFFICIAL INDORSEMENT OR APPROVAL OF THE USE OF SUCH COMMERCIAL HARDWARE OR SOFTWARE.

UNCLASSIFIED

SECURITY CLASSIFICATION OF THIS PAGE (When Data Entered)

REPORT DOCUMENTATION PAGE		READ INSTRUCTIONS BEFORE COMPLETING FORM
1. REPORT NUMBER TE-CR-77-2	2. GOVT ACCESSION NO. (14) DRDMI-TE-CR-77-2	3. RECIPIENT'S CATALOG NUMBER
4. TITLE (and Subtitle) (6) COMPUTER SIMULATION OF TURBULENCE INDUCED POINTING JITTER FOR A LASER DESIGNATOR.		5. TYPE OF REPORT & PERIOD COVERED (7) Technical Report
7. AUTHOR(s) (10) David L. Fried		8. CONTRACT OR GRANT NUMBER(s)
9. PERFORMING ORGANIZATION NAME AND ADDRESS Optical Science Consultants P. O. Box 446 Placentia, California 92670		10. PROGRAM ELEMENT, PROJECT, TASK AREA & WORK UNIT NUMBERS
11. CONTROLLING OFFICE NAME AND ADDRESS Commander US Army Missile Command Attn: DRDMI-TE Redstone Arsenal, Alabama 35809		12. REPORT DATE (11) Mar 76
14. MONITORING AGENCY NAME & ADDRESS (if different from Controlling Office) Commander US Army Missile Command Attn: DRDMI-TI Redstone Arsenal, Alabama 35809		13. NUMBER OF PAGES 21
		15. SECURITY CLASS. (of this report) UNCLASSIFIED
		15a. DECLASSIFICATION/DOWNGRADING SCHEDULE
16. DISTRIBUTION STATEMENT (of this Report) Approved for public release; distribution unlimited.		
17. DISTRIBUTION STATEMENT (of the abstract entered in Block 20, if different from Report)		
18. SUPPLEMENTARY NOTES		
19. KEY WORDS (Continue on reverse side if necessary and identify by block number) Atmospheric turbulence Laser target designator		
20. ABSTRACT (Continue on reverse side if necessary and identify by block number) The statistics of turbulence-induced, angle-of-arrival fluctuations are formulated and presented in a form suitable for computer calculations of the fluctuation power spectrum for the baseline propagation case of an aperture viewing a point source. It is then shown how these results can be applied to the case of a laser target designator of finite aperture size projecting a slightly divergent beam. Representative computer programming is presented ABSTRACT (Continued)		

DD FORM 1 JAN 73 1473 EDITION OF 1 NOV 65 IS OBSOLETE

UNCLASSIFIED
SECURITY CLASSIFICATION OF THIS PAGE (When Data Entered)


410 143.

UNCLASSIFIED

SECURITY CLASSIFICATION OF THIS PAGE(When Data Entered)

ABSTRACT (Concluded)

(written in BASIC). A sample case has been run with results presented. The necessary random signal generation and filtering procedures are described to generate each of the two components of the pointing jitter with statistics matching the calculated power spectrum.



UNCLASSIFIED

SECURITY CLASSIFICATION OF THIS PAGE(When Data Entered)

CONTENTS

	Page
I. INTRODUCTION.	3
II. PROPAGATION FORMULATION	4
III. LASER TARGET DESIGNATOR PROPAGATION GEOMETRY.	6
IV. SAMPLE RESULTS.	9
V. RANDOM JITTER GENERATION.	12
Appendix A. CALCULATION OF THE BASELINE POWER SPECTRUM	15
Appendix B. CALCULATION OF THE POWER SPECTRUM OF EACH COMPONENT.	17
Appendix C. CALCULATION OF THE LASER TARGET DESIGNATOR ATMOSPHERIC TURBULENCE	19

I. INTRODUCTION

In this report, the formalism for calculation of the atmospheric turbulence-induced power spectrum of beam wander for a laser transmitter will be set up. A procedure for generating a random sequence of values corresponding to each component of beam wander will be established. The effect of atmospheric turbulence on a laser target designator will be evaluated.

The temporal statistics of the effects of atmospheric turbulence on the direction of propagation of a laser beam is determined by the laser wave length, λ , the laser transmitter's (i.e., the laser target designator's) aperture diameter, D , the range from the transmitter to the target, R , the distribution of the optical strength of turbulence along the path as measured by the refractive-index structure constant, C_N^2 , and by the distribution along the propagation path of the component of the effective wind velocity perpendicular to the path, V_{eff} . All of these except C_N^2 and V_{eff} are single value parameters. However, C_N^2 and V_{eff} can vary with the position z along the propagation path. It is to be noted that the effective wind velocity, V_{eff} , is not determined entirely by the actual wind velocity, but may contain a component which depends on the angular rate at which the laser beam is being slewed through the air. What really matters is the rate at which a "parcel" of turbulent atmosphere passes through the laser beam.

By virtue of optical antenna gain reciprocity*, the ability to calculate the temporal statistics of the variations in angle-of-arrival can be utilized at an optical receiver aperture to determine the laser beam pointing jitter if that same aperture were functioning as a laser transmitter used to irradiate what before was the optical source.** In this analysis, the designator will be considered a receiver and the target an optical source. The angle-of-arrival temporal statistics will be calculated at the designator-"receiver".

Fortunately, a fairly compact set of theoretical results have recently been developed for the subject of angle-of-arrival temporal

*Fried, D. L. and Yura, H. T., "Telescopic-Performance Reciprocity for Propagation in a Turbulent Medium," J. Opt. Soc. Am., Volume 62, 1972, p. 600.

**Hance, H. V. and Fried, D. L., "experimental Test of Optical Antenna-Gain Reciprocity," J. Opt. Soc. Am., Volume 63, 1973, p. 1015.

statistics.* With this theory, the angle-of-arrival statistics can easily be formulated for a particularly general baseline propagation problem. It is then a matter of geometric argument and simple algebraic manipulation to make this result apply to the propagation geometry of interest in the case of the laser target designator.

In the following section, the existing theory for angle-of-arrival temporal statistics shall be reviewed. In the next section, the geometric arguments will be provided that allow translation of this result to the geometry of the laser target designator problem. After that, a sample numerical problem will be worked. In the final section it will be shown how a suitably designed random pointing error generator might be configured in digital computer simulation to produce a signal matching the calculated temporal statistics.

II. PROPAGATION FORMULATION

A receiver of aperture diameter D , receiving laser radiation of wavelength λ , is considered from a point source at a range R . The direction from the point source to (the center of) the receiver is taken to be the z -axis, letting $z = 0$ at the point source, and $z = R$ at the receiver aperture. This geometry is depicted in Figure 1.

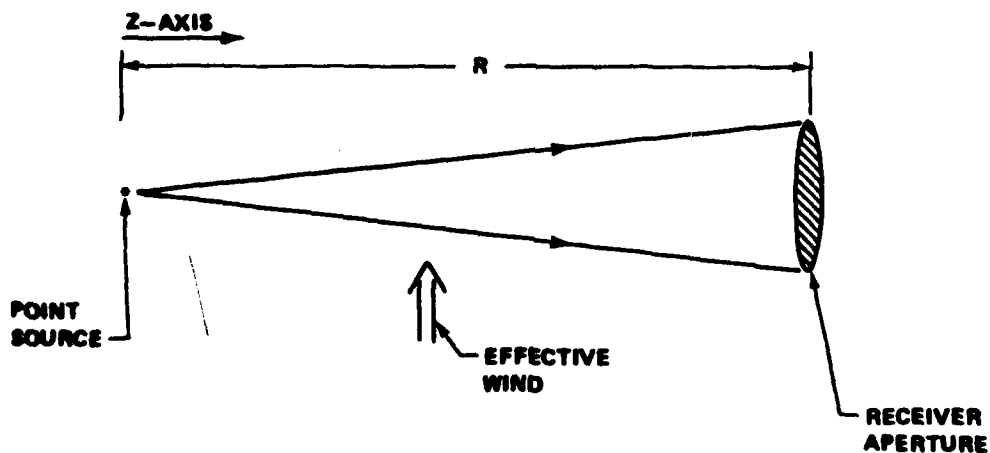


Figure 1. Baseline propagation geometry.

A receiver aperture of diameter D is viewing a point source at range R . The z -axis corresponds to the direction from the point source to the aperture ($z = 0$ at the point source). For the baseline problem, calculation of the angle-of-arrival power spectrum for the wavefront arriving at the aperture from the point source is of interest. The effective wind is, as shown, the component of the wind (and associated beam slew effects) perpendicular to the z -axis.

*Greenwood, D. P. and Fried, D. L., Power Spectra Requirement for Wavefront-Compensative Systems, Rome Air Development Center, AFSC, Griffiss Air Force Base, New York 13441, September 1975, RADC-TR-75-227.

One component of the angle-of-arrival variations of the wavefront as it reaches the receiver aperture, measured in radians shall be denoted by $\alpha(t)$. (Only a single component is necessary because the statistics will be the same for both components and the results will apply equally well to each.) It can be shown that $\alpha(t)$ has zero mean value and stationary statistics. Hence, the angle-of-arrival temporal coherence function can be expressed as

$$C_{\alpha}(\tau) = \langle \alpha(t) \alpha(t + \tau) \rangle \quad (1)$$

where τ denotes time, measured in seconds. The associated power spectrum can be written as

$$F_{\alpha}(f) = 4 \int_0^{\infty} d\tau \cos(2\pi f \tau) C_{\alpha}(\tau) \quad (2)$$

with f denoting temporal frequency, measured in hertz. The fact that $C_{\alpha}(\tau)$ is an even function insures that there is no sine, or imaginary, part to the power spectrum. The calculation of $F_{\alpha}(f)$ will be the basic concern in this section.

It has been shown by Greenwood and Fried* that if the propagation range $z = 0$ to $z = R$ is subdivided into N adequately small regions, of width Δz_i and with midpoints at z_i , where $i = 1$ to N , then the following equations can be written:

$$F_{\alpha}(f) = \sum_{i=1}^N F_{\alpha,i}(f) \quad (3)$$

where

$$F_{\alpha,i}(f) = 1.32 \times 10^{-2} (\lambda/D)^2 (D/r_{o,i})^{5/3} f_{o,i}^{-1/3} f^{-2/3} G_{\alpha}(f/f_{o,i}). \quad (4)$$

The function $G_{\alpha}(f/f_{o,i})$ is defined by the expression

$$G_{\alpha}(f/f_{o,i}) = \begin{cases} 1 & \text{if } 0 \leq f \leq 0.332 f_{o,i} \\ 1.12 - 0.361 (f/f_{o,i}) & \text{if } 0.332 f_{o,i} < f \leq 3.10 f_{o,i} \\ 0 & \text{if } 3.10 f_{o,i} < f \end{cases} \quad (5)$$

*Ibid.

The quantities $r_{o,i}$ and $f_{o,i}$ are determined by the local turbulence and effective wind characteristics in the i^{th} segment of the propagation path. With $C_{N,i}^2$ denoting the refractive-index structure constant in the i^{th} segment, $V_{\text{eff},i}$ denoting the effective wind velocity in the i^{th} segment, z_i denoting the position on the z-axis of the midpoint of the i^{th} segment, and Δz_i denoting the width of the i^{th} segment, the following equations can be written:

$$r_{o,i} = [16.7 \Delta z_i C_{N,i}^2 (z_i/R)^{5/3} / \lambda^2]^{-3/5} \quad (6)$$

and

$$f_{o,i} = \frac{V_{\text{eff},i}}{\pi D (z_i/R)} \quad (7)$$

Equations (3) to (7) provide a straightforward basis for the calculation of angle-of-arrival fluctuations for a receiver viewing a point source.

This constitutes the baseline problem. For purposes of definiteness, a computer program has been prepared in the form of a subroutine for the calculation of the baseline power spectrum. This is listed in Appendix A.

III. LASER TARGET DESIGNATOR PROPAGATION GEOMETRY

The laser target designator has a rather small aperture diameter compared to the diameter of the transmitted laser spot. If the laser target designator diameter is D_T and the angular divergence of the laser beam is θ , then the diameter of the laser spot will be

$$D_S = D_T + \theta R_1 \quad (8)$$

where R_1 is the range from the laser target designator to the laser spot. (The interest here is restricted to the gedanken situation where the laser spot is defined on a virtual screen perpendicular to the z-axis.)

To calculate the angle of arrival fluctuations at the laser spot, the baseline formalism can be utilized, except that it would be assumed that there was a point source located a distance

$$R_2 = D_T / \theta \quad (9)$$

behind the laser target designator aperture. A further assumption is that there is no turbulence in this added region. The geometry of this configuration is depicted in Figure 2. In this virtual formulation, the problem posed is directly reduced to a version of the baseline case.

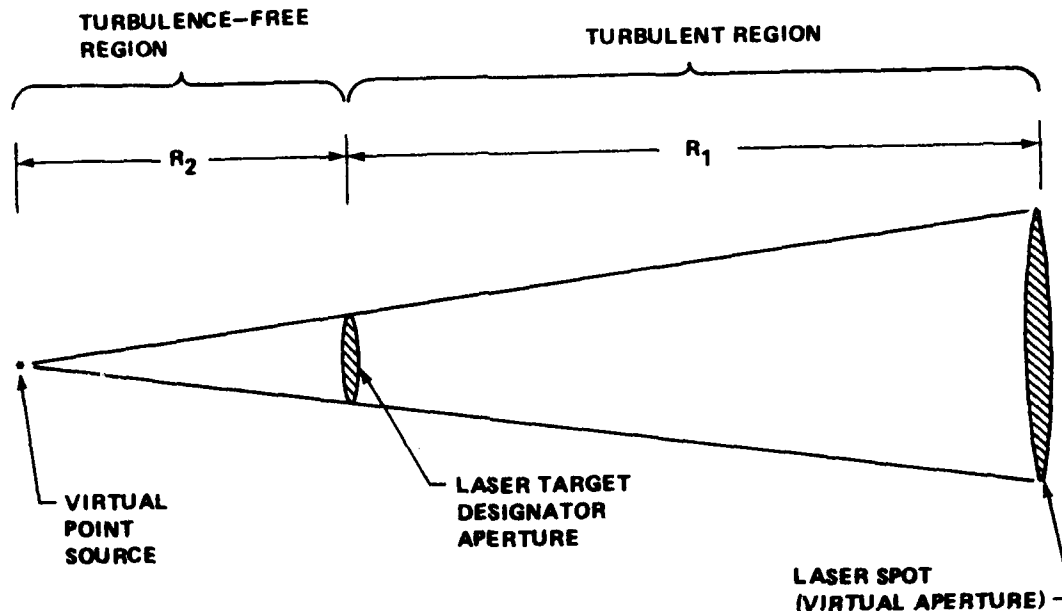


Figure 2. Virtual propagation geometry for laser target designator.

The laser target designator projects a laser spot at range R_1 which, because of the laser beam spread, is considerably larger than the aperture diameter of the laser target designator. The wavefront angle-of-arrival at the laser spot can be evaluated by treating the spot as a virtual aperture viewing a virtual point source located behind the laser target designator. With the laser target designator ignored, and treating the turbulence as being restricted to the R_1 region with the R_2 region being turbulence-free, the problem reduces to the baseline case.

The angle-of-arrival can be analyzed at the laser spot in terms of the baseline formulation by doing the following:

- 1) The baseline parameter D is taken to be

$$D = D_s \quad . \quad (10)$$

- 2) The baseline parameter R is taken to be

$$R = R_1 + R_2 \quad . \quad (11)$$

3) The propagation path in the baseline case is taken to be subdivided into $N + 1$ regions $i = 0$ to N , with the $i = 0$ segment having a width

$$\Delta z_1 = R_2, \quad \text{for } i = 0, \quad (12)$$

and a refractive index structure constant

$$C_{N,i}^2 = 0, \quad \text{for } i = 0. \quad (13)$$

4) For the part of the propagation path corresponding to R_1 , the values of N , Δz_i , and $C_{N,i}^2$ are taken in the same manner if the propagation path were just over the length R_1 .

5) The values of z_i are taken to be those which would be obtained if the propagation path were just over R_1 , except that R_2 is added to each value; thus,

$$z_i = R_2 + \sum_{j=1}^{i-1} \Delta z_j + 1/2 \Delta z_i. \quad (14)$$

6) In the actual wind perpendicular to the z -axis in the i^{th} section is $V_{\perp,i}$, and the laser target designator is slewing at an angular rate $\dot{\theta}$, then the following equation results:

$$V_{\text{eff},i} = V_{\perp,i} \pm \dot{\theta} (z_i - R_2), \quad (15)$$

where the plus or minus sign is chosen accordingly as the angular slew direction is opposed to or parallel to the sense of $V_{\perp,i}$.

With these substitutions and using the algorithm of the baseline case as represented in the subroutine of Appendix A, the power spectrum of each component of the angle-of-arrival of the wave-front can be calculated from a point source as it reaches the laser spot position in accordance with the problem definition in Figure 2. It is a straightforward matter to set up a computer subroutine for this calculation. This is done in Appendix B, but first one further matter must be noted.

Having determined the angle-of-arrival fluctuation statistics at the laser spot, reciprocity arguments^{*,**} can now be applied the same results as the statistics of beam pointing variations when the laser spot is a laser transmitter of diameter D_3 transmitting a beam focused

*Op. Cit., Fried and Yura.

**Op. Cit., Hance and Fried.

on the position of the virtual point source at range $R_1 + R_2$. The power spectrum of pointing jitter at the laser spot position is identical with what would be calculated for the angle-of-arrival spectrum. Now, considering the laser spot position as the transmitter, the angle-of-arrival spectrum of the partially converged but not fully focused beam can be investigated when it reaches the position of the laser target designator. It can be shown through any of several arguments that the angle-of-arrival power spectrum at the laser target designator position is just $(D_S/D_T)^2$ times the beam pointing jitter and thus times the angle-of-arrival jitter at the laser spot position. The simplest argument for this follows from the LaGrange invariant which requires that in a passive optical system (which is what the turbulent atmosphere is at any instant) angle times aperture (i.e., beam) diameter at one position in the system must equal angle times aperture (i.e., beam) diameter at any other position in the system. Because the angle-of-arrival power spectrum is proportional to angle squared, the ratio of diameters squared is utilized; hence the $(D_S/D_T)^2$ factor.

It is immediately obvious from reciprocity considerations that the pointing jitter induced turbulence in the laser target designator transmitting a beam to the laser spot is also equal to $(D_S/D_T)^2$ times the angle-of-arrival spectrum at the laser spot position of the wavefront from the virtual point source: The formalism for calculating this latter quantity was set up in the first part of this section. In Appendix B, this formalism is utilized to allow calculation of the laser target designator turbulence induced pointing jitter power spectrum.

IV. SAMPLE RESULTS

With the capabilities defined by the programs in Appendices A and B, a set of sample results can be calculated. In this section, first a sample calculation of the power spectrum shall be performed and then it will be shown how this results can be used to generate an appropriate random sample of a time varying laser target designator pointing jitter.

A problem is considered in which the laser target designator is operating at a wavelength of $\lambda = 1.06 \times 10^{-6}$ m, has an aperture diameter of $D_T = 0.04$ m, and is illuminating a target at a range $R_1 = 3 \times 10^3$ m. The laser beam spread (full angle) is $\theta = 5 \times 10^{-4}$ rad; the target is assumed to be moving at a crossing velocity, i.e., a velocity perpendicular to the line of sight of 25 km/hour (6.94 m/sec). At a 3-km

range, this gives rise to a beam slewing angular rate of $\dot{\theta} = 2.31 \times 10^{-3}$ rad/sec. It is assumed that the propagation is between two hills and across a valley so that the strength of turbulence is lowest at the center of the path and approximately equally higher at both ends; the wind velocity is lowest at the two ends and highest at the center.

The propagation path shall be considered to be subdivided into $N = 10$ equal length segments, so that the segment length are $\Delta z_i = 300$ m ($i = 1, 2, \dots, 10$). The refractive-index structure constant is taken to vary between $10 \times 10^{-14} \text{ m}^{-2/3}$ at the two ends of the path to $2 \times 10^{-14} \text{ m}^{-2/3}$ at the center of the path. Explicitly, the following equations are set:

$$\begin{aligned} C_{N,1}^2 &= C_{N,10}^2 = 10 \times 10^{-14} , \\ C_{N,2}^2 &= C_{N,9}^2 = 7 \times 10^{-14} , \\ C_{N,3}^2 &= C_{N,8}^2 = 5 \times 10^{-14} , \\ C_{N,4}^2 &= C_{N,7}^2 = 3 \times 10^{-14} , \\ C_{N,5}^2 &= C_{N,6}^2 = 2 \times 10^{-14} . \end{aligned} \quad (16)$$

The actual wind velocity component perpendicular to the propagation path is taken to vary between 10 m/sec near the center of the path to 3 m/sec near the two ends of the propagation path (i.e., between approximately 22 mph and 7 mph). Explicitly, the following equations are set:

$$\begin{aligned} V_{\perp,1} &= V_{\perp,10} = 3 \text{ m/sec} , \\ V_{\perp,2} &= V_{\perp,9} = 6 \text{ m/sec} , \\ V_{\perp,3} &= V_{\perp,8} = 8 \text{ m/sec} , \\ V_{\perp,4} &= V_{\perp,7} = 9 \text{ m/sec} , \\ V_{\perp,5} &= V_{\perp,6} = 10 \text{ m/sec} . \end{aligned} \quad (17)$$

These values completely define the propagation problem.

A computer run has been set up using the DATA instructions shown in Appendix C to calculate the laser target designator atmospheric turbulence induced pointing jitter for the $M = 9$ (logarithmically uniformly spaced) frequencies of $f = 0.1, 0.1778, 0.3162, 0.5623, 1.000, 1.778, 3.162, 5.623, \text{ and } 10.00$ Hz. The results of this calculation are shown in Appendix C and graphed in Figure 3.

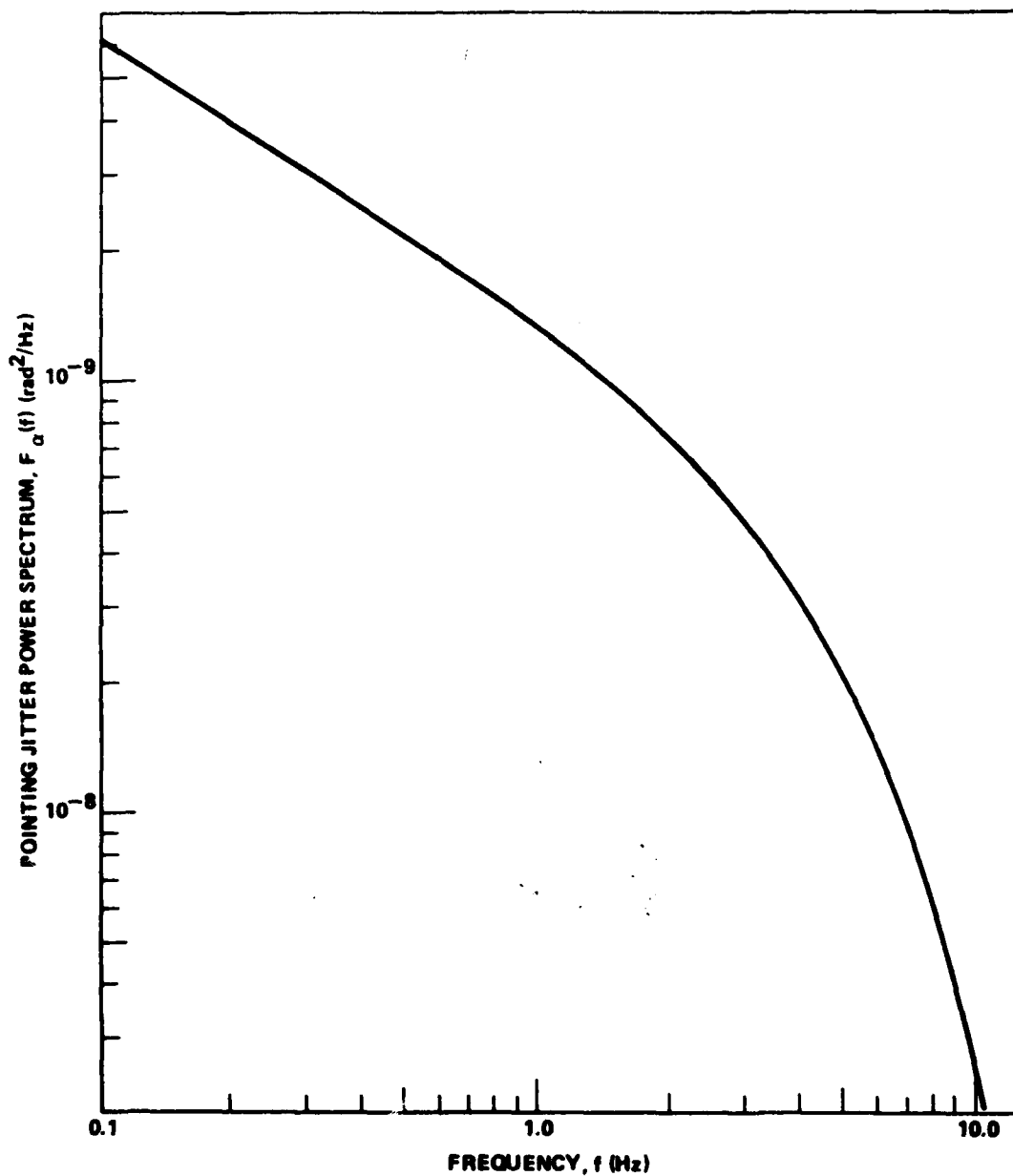


Figure 3. Laser target designator pointing jitter power spectrum.

Pointing jitter is induced by the turbulence and wind speed distribution given as an example in the test. The complete set of problem parameters are specified by the "DATA" statements given in Appendix C. The computation of the power spectrum was carried out using the programs in Appendices A and B.

V. RANDOM JITTER GENERATION

The problem now is to find a means of easily generating a random sequence with this power spectrum. It is suggested that the simplest way to do this is to define a set of simple digital R-C low pass 6-dB/octave filters which when summed will have a transfer function equal to the square root of the pointing jitter power spectrum. If a random white noise is put into such a network, the output will be random noise with the appropriate power spectrum. The matter of scaling will be discussed shortly, but first the generation in a computer simulation of the random white noise and the formulation of the appropriate R-C network in the computer will be discussed.

For all of the computer work, a $\Delta t = 0.001$ sec time increment will be utilized. This means that frequencies up to $(2\Delta t)^{-1} = 500$ Hz can be handled and frequencies up to approximately 100 Hz can be handled adequately.* A random sequence of gaussianly distributed independent random values with unity variance is generated associating each one with a sequence of time intervals Δt , then the resultant signal will appear to be white noise with unity variance and a power spectrum that is abruptly truncated at the Nyquist frequency, $f_N = (2\Delta t)^{-1}$. Because the variance of a random signal equals the integral of the power spectrum over the frequency range 0 to ∞ , it follows that the power spectral density of this white noise is

$$N_o = 1/f_N = 2\Delta t \quad (18)$$

A single R-C low pass digital filter is digitally implemented in accordance with Figure 4. Here the box labeled " z^{-1} " denotes a time delay between input and output of one cycle time, Δt . If the factor k is chosen to be

$$k = \exp(-2\pi f_{RC} \Delta t) \quad (19)$$

and the factor K is chosen to be

$$K = 1 - k \quad (20)$$

then in the limit of sample data approximations, the output signal will appear to be the input signal filter by an R-C low pass filter with the knee of its transfer function at f_{RC} . It is noted that this filter has

*If higher frequencies are required, it is merely necessary to use a smaller value for Δt .

unity gain, i.e., if a dc signal is input, the output will be a dc signal of the same amplitude. The transfer function of this filter will be denoted by $Y(f_{RC}; f)$. A set of these filters will be summed; each with separate f_{RC} and separate weighting factor, A , so as to obtain a composite transfer function $Y_{Tot}(f)$, whose magnitude squared will approximate the pointing jitter power spectrum in Figure 4.

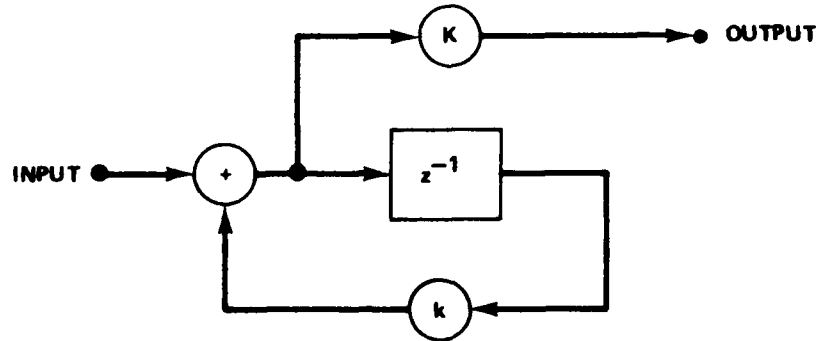


Figure 4. Recursive filter design for digital computer simulation of an R-C low pass filter.

The box labeled z^{-1} denotes a single time delay of duration Δt . To obtain a unity gain filter with the knee of its transfer function at f_{RC} , the multiplicative constants k and K are set equal to $\exp(-2\pi f_{RC} \Delta t)$ and $1 - \exp(-2\pi f_{RC} \Delta t)$, respectively.

Thus, the following equation can be written:

$$Y_{Tot}(f) = \sum_{j=1}^J A_j Y(f_{RC,j}; f) , \quad (21)$$

and

$$|Y_{Tot}(f)|^2 \approx \text{Power Spectrum of Figure 3} . \quad (22)$$

The value of J is chosen to allow reasonably accurate approximation in Equation (22). (Care is required in the choice of the A_j 's and $f_{RC,j}$'s to insure a good approximation.)

Now if the sequence of unity variance random values is multiplied by N_0^{-1} and passed through the filter $Y_{Tot}(f)$, the output will have the statistics of the laser target designator turbulence induced pointing jitter.

Appendix A. CALCULATION OF THE BASELINE POWER SPECTRUM

```

1000 REM
1001 REM THIS PROGRAM, WRITTEN IN BASIC WILL CALCULATE
1002 REM THE POWER SPECTRUM OF THE ANGLE-OF-ARRIVAL FOR
1003 REM THE BASELINE CASE OF AN APERTURE VIEWING A POINT
1004 REM SOURCE. THE PROGRAM FUNCTIONS AS A SUBROUTINE,
1005 REM AND IS ENTERED WITH THE FOLLOWING PARAMETERS SET,
1006 REM
1007 REM L=LASER WAVELENGTH, LAMRDA
1008 REM D=APERTURE DIAMETER
1009 REM R=PROPAGATION PATH LENGTH
1010 REM F=FREQUENCY FOR WHICH THE POWER SPECTRUM
1011 REM IS TO BE EVALUATED
1012 REM N=NUMBER OF SEGMENTS IN THE PROPAGATION
1013 REM PATH
1014 REM Z(I)=RANGE FROM BASELINE CASE POINT SOURCE
1015 REM TO THE MIDPOINT OF THE I-TH SEGMENT
1016 REM Z1(I)=LENGTH OF THE I-TH SEGMENT
1017 REM C(I)=C-SUB-N SQUARED FOR THE I-TH SEGMENT
1018 REM V(I)=V-SUB-EFF FOR THE I-TH SEGMENT
1019 REM
1020 REM THE SUBROUTINE IS EXITED WITH
1021 REM
1022 REM F1=VALUE OF THE POWER SPECTRUM FOR FREQUENCY F.
1023 REM
1024 REM
1050 LET F1=0
1055 FOR I=1 TO N
1060 LET F0=V(I)/(3.14159*D*Z(I)/R)
1065 LET R0=(16.7*Z1(I)*C(I)*(Z(I)/R)+1.66667/(L*L))^(-.6)
1070 IF F<=.332*F0 LET G=1
1075 IF F>.332*F0 IF F<=3.1*F0 LET G=1.12-.361*F/F0
1080 IF F>3.1*F0 LET G=0
1085 LET F1=F1+1.32E-02*(L/D)+2*((D/R0)+5/(F*F*F0))+.333333*G
1090 NEXT I
1095 RETURN

```

Appendix B. CALCULATION OF THE POWER SPECTRUM OF EACH COMPONENT

```

100 REM
101 REM   THIS PROGRAM, WRITTEN IN BASIC WILL CALCULATE THE
102 REM   POWER SPECTRUM OF EACH COMPONENT OF ATMOSPHERIC
103 REM   TURBULENCE INDUCED POINTING JITTER OF A LASER
104 REM   TARGET DESIGNATOR. THE PROGRAM MAKES USE OF THE
105 REM   SUBROUTINE IN APPENDIX A. THE PROGRAM IS STARTED
106 REM   WITH THE PARAMETERS DEFINING THE PROBLEM SITUATION
107 REM   AND THE NATURE OF THE REQUIRED RESULTS GIVEN BY
108 REM   A SET OF "DATA" STATEMENTS. AS LISTED HERE THESE
109 REM   "DATA" STATEMENTS ARE FILLED WITH ZEROS. FOR ACTUAL
110 REM   PROGRAM OPERATION THESE ZERO VALUES HAVE TO BE
111 REM   REPLACED BY THE APPROPRIATE VALUES.
112 REM
113 REM   LINE 150 IS A "DATA" STATEMENT LISTING IN ORDER
114 REM   THE VALUES OF THE FOLLOWING:
115 REM       L=LASER WAVELENGTH, LAMBDA (IN METERS)
116 REM       D1=LASER TARGET DESIGNATOR APERTURE DIAMETER,
117 REM           D-SUB-T (IN METERS)
118 REM       T=LASER BEAM SPREAD, THETA (IN RADIANS)
119 REM       T1=LASER BEAM SLEW RATE, THETA-DOT (IN
120 REM           RADIANS PER SECOND)
121 REM       R1=PROPAGATION RANGE FROM THE LASER TARGET
122 REM           DESIGNATOR TO THE LASER SPOT, R-SUB-1
123 REM           (IN METERS)
124 REM
125 DATA 0,0,0,0,0
155 READ L
156 READ D1
157 READ T
158 READ T1
159 READ R1
160 LET D2=D1+T*R1
161 LET R2=D1/T
165 REM
166 REM   LINE 190 AND THE IMMEDIATELY FOLLOWING LINES ARE
167 REM   "DATA" STATEMENTS GIVING IN ORDER THE VALUES OF
168 REM   THE FOLLOWING:
169 REM       N=NUMBER OF SEGMENTS THE PROPAGATION PATH IS
170 REM           CONSIDERED TO BE DIVIDED INTO FOR THE
171 REM           COMPUTATION
172 REM       Z1(I)=A SET OF N-VALUES CORRESPONDING TO THE
173 REM           LENGTH OF THE I-TH SEGMENT, DELTA-Z-
174 REM           SUB-1 (IN METERS)
175 REM       C(I)=A SET OF N-VALUES OF THE REFRACTIVE-INDEX
176 REM           STRUCTURE CONSTANT IN THE I-TH SEGMENT,
177 REM           C-SUB-N-SQUARED-SUB-1 (IN METERS2/3)
178 REM       V1(I)=A SET OF N-VALUES OF THE ACTUAL WIND VELOCITY
179 REM           PERPENDICULAR TO THE PROPAGATION DIRECTION
180 REM           IN THE I-TH SEGMENT, V-SUB-PERPENDICULAR
181 REM           (IN METERS PER SECOND)
182 REM

```

```

190 DATA 0
191 DATA 0,0,0,0,0,0,0,0,0,0
192 DATA 0,0,0,0,0,0,0,0,0,0
193 DATA 0,0,0,0,0,0,0,0,0,0
200 READ N
205 DIM Z1(N),Z(N),C(N),V(N)
210 LET Z=R2
215 LET Z1=0
220 FOR I=1 TO N
225 READ Z1(I)
230 LET Z=Z+.5*(Z1+Z1(I))
235 LET Z(I)=Z
240 LET Z1=Z1(I)
245 NEXT I
250 FOR I=1 TO N
255 READ C(I)
260 NEXT I
265 FOR I=1 TO N
270 READ V1
275 LET V(I)=V1+T1*(Z(I)-R2)
280 NEXT I
285 REM
286 REM      LINE 300 AND THE LINES IMMEDIATELY FOLLOWING ARE
287 REM      "DATA" STATEMENTS SPECIFYING THE FOLLOWING:
288 REM      M=THE NUMBER OF FREQUENCIES FOR WHICH THE
289 REM      POINTING JITTER POWER SPECTRUM IS TO
290 REM      CALCULATED
291 REM      F(I)=A SET OF M-VALUES CORRESPONDING TO THE
292 REM      VARIOUS FREQUENCIES FOR WHICH THE POWER
293 REM      SPECTRUM IS TO BE CALCULATED (IN HERTZ).
294 REM
300 DATA 0
301 DATA 0,0,0,0,0,0,0,0,0,0
305 READ M
310 DIM F(M)
315 FOR I=1 TO M
320 READ F(I)
325 NEXT I
330 REM
331 REM      ALL OF THE PROBLEM PARAMETERS ARE ESTABLISHED AT
332 REM      THIS POINT. THE PROGRAM NOW SETS UP THE VARIOUS
333 REM      PARAMETERS TO CALL THE SUBROUTINE, AND AFTER EACH
334 REM      CALL PRINTS OUT THE RELEVANT RESULTS.
335 REM
340 LET D=D2
345 LET R=R1+R2
350 FOR J=1 TO M
355 LET F=F(J)
360 GOSUB 1000
365 LET F1=F1*(D2/D1)+2
370 PRINT "FREQUENCY = ";F; TAB (25);"POWER SPECTRUM = ";F1
375 NEXT J

```

BEST AVAILABLE COPY

Appendix C. CALCULATION OF THE LASER TARGET DESIGNATOR ATMOSPHERIC TURBULENCE

In the text, a sample problem was set up for evaluation. Here, the appropriate DATA statements for the problem and then the computed power spectrum are exhibited in place of the empty DATA statements of Appendix B as follows:

150 DATA 1.06E-6, 4E-2, 5E-4, 2.31E-3, 3E3

190 DATA 10

191 DATA 300, 300, 300, 300, 300, 300, 300, 300, 300, 300

192 DATA 1E-13, 7E-14, 5E-14, 3E-14, 2E-14

193 DATA 2E-14, 3E-14, 5E-14, 7E-14, 1E-13

194 DATA 3, 6, 8, 9, 10, 10, 9, 8, 6, 3

300 DATA 9

301 DATA 0.1, 0.1778, 0.3162, 0.5623, 1.0, 1.778, 3.162, 5.623, 10.0

Line 150 gives λ , D_T , θ , $\dot{\theta}$, and R_1 , in that order. Line 190 says that the propagation range is divided into 10 intervals. Line 191 gives the value of Δz_i for each of the 10 intervals. Line 192 gives the value of $C_{N,i}^2$ for each of the 10 intervals. Line 193 gives the values of $V_{L,i}$ for each of the 10 intervals. Line 300 says that the power spectra will be computed for 9 frequencies. Line 301 gives the values of the 9 frequencies.

Using the programs in Appendices A and B, and the preceding DATA statements, the following results were calculated. These results are plotted in Figure 3.

FREQUENCY =	.1	POWER SPECTRUM =	6.12732E-08
FREQUENCY =	.1778	POWER SPECTRUM =	4.17496E-08
FREQUENCY =	.3162	POWER SPECTRUM =	2.84413E-08
FREQUENCY =	.5623	POWER SPECTRUM =	1.93775E-08
FREQUENCY =	1	POWER SPECTRUM =	1.28571E-08
FREQUENCY =	1.778	POWER SPECTRUM =	7.89682E-09
FREQUENCY =	3.162	POWER SPECTRUM =	4.24644E-09
FREQUENCY =	5.623	POWER SPECTRUM =	1.50639E-09
FREQUENCY =	10	POWER SPECTRUM =	2.46497E-10

DISTRIBUTION

	No. of Copies		No. of Copies
Defense Documentation Center Cameron Station Alexandria, Virginia 22314	12	Director Benet Weapons Laboratory Watervliet Arsenal Attn: SWEV-RDD-SE, Mr. Andrade Watervliet, New York 12189	1
Commander US Army Electronics Command Attn: DRSEL-CT-L, Dr. Buser	1	Chief, Missile EW Technical Area US Army Electronic Warfare Laboratory Attn: DRSEL-WL-M	1
VL-E, Mr. Flynn	1	MJ, Mr. Kasperek	1
CT-L-A, Mr. Mirachi	1	WL-MS, Sylvia Hoi jelle	1
WL-D, Mr. Hardin	1	White Sands Missile Range, New Mexico New Mexico 88002	
WLN, Mr. Giambalvo	1		
WLS, Mr. Charlton	1		
Fort Monmouth, New Jersey 07703			
Commander US Army Armaments Command Attn: SARML-LR, Dr. Amoroso	1	Director, US Army Materials and Mechanics Research Center Attn: DRXMR-HH, Mr. Digham	1
-T-SFA, Mr. Fosbinder	1	Watertown, Massachusetts 02172	
DRCPH-CANS, COL S. T. Post, Jr.	1	Director, Harry Diamond Laboratories Attn: DRXDO-RCB, Dr. Gleason	1
Rock Island, Illinois 61201		SAB, Mr. Johnson	1
Commander US Army Materiel Command Attn: DRCRD-MT-MT	5	Connecticut Ave and Van Ness Street, NW Washington, DC 20438	
5001 Eisenhower Avenue Alexandria, Virginia 22304		Commander US Marine Corps Development and Education Command Attn: Development Center	1
Director US Army Materiel Systems Analysis Agency Attn: DREXT-D	1	Quantico, Virginia 22134	
-CS, Mr. Marchetti	1	Commandant US Marine Corps, Code AX Washington, DC 20380	1
Aberdeen Proving Ground, Maryland 21005		Director Waterways Experiment Station Corps of Engineers Attn: Mr. Grabau	1
Commander Edgewood Arsenal Attn: SARMA-TD	1	Dr. LaGarde	1
-DE-DD, Mr. Tannenbaum	1	PO Box 631 Vicksburg, Mississippi 39180	
Aberdeen Proving Ground, Maryland 21010		Commandant US Army Infantry School Attn: ATSH-I	1
Director US Army Air Mobility Research and Development Laboratory Eustis Directorate Attn: SAVDL-BU-MD, Mr. Joe Ladd	1	Fort Benning, Georgia 31905	
Fort Eustis, Virginia 23604		Commandant US Army Armor School Attn: ATSE-CD-M	1
Director Night Vision Laboratory (USASCOM) Attn: DRSEL-MV-VI, Mr. Rodak	1	Fort Knox, Kentucky 40121	
Fort Belvoir, Virginia 22060		Commandant US Army Air Defense School Air Defense Agency Attn: ATSA-CTD-MS	1
Commander US Army Mobility Equipment Research and Development Center Attn: STSFB-SA, Mr. Atkison	1	Fort Bliss, Texas 79916	
Fort Belvoir, Virginia 22060		Commandant US Army Ordnance Center and School Attn: ATSL-CTD-MS-R (LT Roberts)	1
Director Atmospheric Sciences Laboratory (USASCOM) Attn: DRSEL-ML, Mr. Lindberg	1	Aberdeen Proving Ground, Maryland 21005	
White Sands Missile Range, New Mexico 88002		Commander US Army Combined Arms Combat Development Activity Attn: ATCAC-TH	2
Commander Picatinny Arsenal Attn: SETH-AD-C, Mr. Heinemann	1	-E, Mr. Bray	1
FEL, FTRD, Mr. Novak	1	Fort Leavenworth, Kansas 66027	
Dover, New Jersey 07801		Commander US Army Combat Development Experimentation Command Attn: Tech Library - Box 22	1
Commander Frankford Arsenal Attn: SARA-L3000, Dr. McNeill	1	Fort Ord, California 93941	
Philadelphia, Pennsylvania 19137			
Library US Army War College Carlisle Barracks, Pennsylvania 17013	1		

BEST AVAILABLE COPY

No. of Copies

No. of Copies

Headquarters
US Army Foreign Science
and Technology Center
Attn: DRXSP-CBI, Mr. Pearson 2
220 Seventh Street, NE
Charlottesville, Virginia 22901

Headquarters
Department of the Army
The Pentagon
Attn: DARD-DDM, MAJ Kopsac 5
Washington, DC 20310

AFATL/DLWS
Attn: MAJ D. Couture
Eglin Air Force Base, Florida 32542

Defense Advanced Research
Project Agency
Tactical Technology Office
Attn: Dr. C. H. Church 1
1400 Wilson Boulevard
Arlington, Virginia 22209

Commander
Maverick Systems Project Office
Attn: ASD/SD 6SM
65-ENTX
Commander
Naval Weapons Center
Attn: Mr. C. P. Smith (Code 504) 1
Mr. L. W. Nichols (Code 60401) 1
China Lake, California 93555

Dr. Richard E. Schwartz
DDR&E
Office of Assistant for Land Warfare 1
Pentagon, Room 3E1025
Washington, DC 20301

Naval Air Systems Command
Attn: LT CMD F. G. Woods
AIR-5109C, Room 1258JP2
Washington, DC 20360

Headquarters, USAF (RDPA)
Director of Dev. & Acq. DCS/R&D
Attn: LTC Bill Seufert 1
Washington, DC 20330

Headquarters, Air Force Systems Command
Attn: AFSC DLCAW/Mr. R. Cross 1
Andrews Air Force Base
Washington, DC 20334

Air Force Special Communications
Center
Technical Sensors Division
San Antonio, Texas 78243

Director
US Army Ballistic Research Laboratories
Attn: DRXBR-CA (Mr. H. L. Reed) 1
DRXBR-CAL (Mr. Arthur LaGrange) 1
DRXSY, Mr. T. Dolce 1
Aberdeen Proving Ground, Maryland 21005

Director
US Army Human Engineering Laboratory
Attn: DRXHE (Mr. Richard R. Kramer) 1
Aberdeen Proving Ground, Maryland 21005

Commander
Headquarters, US Army Training & Doctrine
Command
Attn: DCS-CD (ATCD-CS-PL) 1
(ATCD-CS-PT) LTC Davis 1
Fort Monroe, Virginia 23615

Headquarters HASSTER
Attn: AFMAS-CSS (Mr. Kirkwood) 1
-AC-PE3 (MAJ Alexander) 1
Fort Hood, Texas 76544

Commander
Naval Weapons Laboratory
Attn: Mr. George Williams, Code EJP
Mr. William Spicer, Code EJM
Dahlgren, Virginia 22448

Commandant
US Army Field Artillery School
Attn: ATSF-CTD-WS
-S
Fort Sill, Oklahoma 73503

DRSHI-FR, Mr. Stickland 1
-LP, Mr. Voigt 1
-V, MAJ Harborth 1
-TRADOC-LNO 1
-YDR, Mr. Todd 1

DRDMI-D 1
-QR, Mr. G. J. Murcheson 1
-X, Dr. McDaniel 1
-T, Dr. Kobler 1
-TD 1
-TE, Mr. Lindberg 1
Mr. Pittman 1
-TEO, Mr. Sittin 1
Mr. Widenhofer 1
Mr. Farmer 1
Mr. Anderson 5
Dr. Emmons 1
-C, MAJ W. Ward 1
MAJ W. Adams 1
CP J. deBlasiere 1
LTC N. Moore 1
Mr. Steven Johnston 1
Mr. H. Osvelt 1
Mr. J. Jernigan 1

-TG 1
-TGT, Mr. Leonard 1
-TK, Dr. Wharton 1
-TL 1
-TRD, Dr. Lilly 5
-ET 1
-TB 3
-TI (Record Set) 1
(Reference Copy) 1

SEARCHED
SERIALIZED
INDEXED
FILED

DISTRIBUTION/AVAILABILITY CODES

Dist.	Avail.	and Special
A		